# Miscibility, Specific Interactions, and Self-Assembly Behavior of Phenolic/Polyhedral Oligomeric Silsesquioxane Hybrids

YUAN-JYH LEE,[1] SHIAO-WEI KUO,[1] WU-JANG HUANG,[2] HUNG-YEN LEE,[1] FENG-CHIH CHANG[1]

[1]Institute of Applied Chemistry, National Chiao-Tung University, Hsin-Chu, Taiwan

[2]Department of Environmental Science and Engineering, National Ping-Tung University of Science and Technology, Ping-Tun, Taiwan

*Received 25 June 2003; revised 27 August 2003; accepted 5 October 2003*

**ABSTRACT:** The miscibility of a phenolic resin with polyhedral oligomeric silsesquioxane (POSS) hybrids and the specific interactions between them were investigated with Fourier transform infrared (FTIR) spectroscopy and wide-angle X-ray diffraction (WAXD). An analysis of the morphology and microstructure was performed with polarized optical microscopy and atomic force microscopy (AFM). The interassociation equilibrium constant between the phenolic resin and POSS (38.7) was lower than the self-association equilibrium constant of pure phenolic (52.3) according to the Painter–Coleman association model. This result indicated that POSS was partially miscible with the phenolic resin. A polarized optical microscopy image of a phenolic/POSS hybrid material (20 wt % POSS) indicated that the crystals of POSS were arranged evenly in the phenolic matrix; the self-assembled array of POSS crystals was also confirmed by AFM. This phenomenon was consistent with the FTIR spectroscopy and WAXD analyses. © 2004 Wiley Periodicals, Inc. J Polym Sci Part B: Polym Phys 42: 1127–1136, 2004
**Keywords:** phenolic; polyhedral oligomeric silsesquioxane (POSS); two-dimensional (2D) Fourier transform infrared (FTIR) spectroscopy; blend

## INTRODUCTION

Because of the length scales of the constituents involved, nanocomposite materials possess extensive interfacial interactions that can affect their salient properties. A novel class of organic–inorganic hybrid materials based on polyhedral oligomeric silsesquioxane (POSS) has been developed in recent years through the copolymerization of the POSS comonomer.[1–11] *POSS* is the term used for compounds having an inorganic $Si_8O_{12}$ core surrounded by seven or eight organic hydrocarbon groups bearing a unique functional group that can undergo polymerization. Most inorganic silicas or creamers are immiscible in general organic systems because of the weak specific interactions in these organic–inorganic hybrids. To improve the properties and miscibility of hybrid materials, it is usually necessary to ensure that favorable specific interactions exist between these components, such as hydrogen bonding, dipole–dipole interactions, and acid–base complexation.

In a previous study, we found that a series of poly(vinyl phenol-*co*-vinylpyrrolidone-*co*-polyhedral oligomeric silsesquioxane) copolymers had glass-transition temperatures significantly greater than those of their corresponding POSS-lacking poly(vinyl phenol-*co*-vinylpyrrolidone) copolymers be-

*Correspondence to:* F.-C. Chang (E-mail: changfc@cc.nctu.edu.tw)

Journal of Polymer Science: Part B: Polymer Physics, Vol. 42, 1127–1136 (2004)

cause of the strong hydrogen-bonding interactions existing between poly(vinyl phenol) and POSS.[12] The exact nature and magnitude, however, of the strength of the hydrogen bonding between POSS and hydrogen-bond-donating polymers have yet to be identified clearly. We have also reported previously that phenolic resins can undergo intermolecular hydrogen bonding in their interactions with hydroxyl, carbonyl, ester, and ether functional groups.[13,14] For convenience, we chose to blend a phenolic resin with POSS to investigate the miscibility, specific interactions, and microstructures.

Fourier transform infrared (FTIR) spectroscopy is commonly used to identify the interactions between different components. This tool can be used both qualitatively and quantitatively to study the mechanism of interpolymer miscibility through the formation of hydrogen bonds. In addition, generalized two-dimensional (2D) correlation spectroscopy, proposed by Noda and coworkers in 1986,[15–17] has been widely applied to polymer science in recent years. This novel method allows the investigation of specific interactions between polymer chains by the measurement of the spectral fluctuations as a function of time, temperature, pressure, and composition. 2D infrared (IR) correlation spectroscopy can identify intramolecular or intermolecular interactions through selected bands in the one-dimensional vibration spectrum. In this study, we used generalized 2D IR correlation spectroscopy to explore the hydrogen-bonding sites in phenolic/POSS hybrids.

The hydrogen-bonding interaction has been described widely in terms of the Painter–Coleman association model (PCAM).[18] The equilibrium constants for hydrogen bonding by self-association ($K_B$) and interassociation ($K_A$), based on PCAM, can be obtained because FTIR spectroscopy allows the fraction of hydrogen-bonded functional groups to be determined. An important feature of this model is that when interassociation is strongly favored over self-association, the polymer blend is expected to be miscible. Conversely, if self-association is stronger than interassociation, the blend tends to be immiscible or partially miscible. In addition, the Si—O—Si bond interaction of POSS also can be calculated from isolating behavior to significant coupling. Molecular orbital calculations have been carried out on the Si—O—Si bridge of zeolites, including $Ag^+$, $Na^+$, and other cations. Given the known structure of the silicate framework, the highest occupied molecular orbitals and lowest unoccupied molecular orbitals have been studied computationally, and the oscillator strength has been calculated for the electronic transition interactions between hetero atoms, as reported by Calzaferri and coworkers.[19–22] In this study, we focus on PCAM, which indicates that the interassociation equilibrium constant between phenolic and POSS is lower than the self-association equilibrium constant of pure phenolic. Thus, partial miscibility may occur in this phenolic/POSS hybrid. The self-assembly of POSS crystals into organized arrays was made apparent by wide-angle X-ray diffraction (WAXD), polarized optical microscopy, and atomic force microscopy (AFM). The phenolic resin limits POSS crystal growth, and the dimension of the resulting crystals is narrow in its distribution (1.5–2.0 $\mu$m).

## EXPERIMENTAL

### Sample Preparation

The novolac-type phenolic resin was synthesized by a condensation reaction with sulfuric acid. The number-average and weight-average molecular weights of the phenolic resin were 500 and 1200 g/mol, respectively. POSS bearing eight isobutyl hydrocarbon groups was purchased from Aldrich. Tetrahydrofuran (THF) and other solvents were predried over molecular sieves before use.

### Phenolic/POSS Hybrids

The phenolic resin and various amounts of POSS were mixed in THF (5%) and stirred for 2 h at room temperature and were then poured into a Teflon disk. The solvent in the Teflon disks was evaporated slowly at room temperature for 12 h, and the hybrid films were then dried at 80 °C *in vacuo* for 24 h. The hybrid material was annealed at 100 °C for 2 h before characterization.

### Characterization

#### *IR Spectroscopy*

IR spectroscopy measurements were performed with a Nicolet Avatar 320 FTIR spectrophotometer from 4000 to 400 $cm^{-1}$ at a resolution of 1.0 $cm^{-1}$. The sample preparation was conducted under a continuous flow of nitrogen to minimize any oxidation or degradation. For a sample analyzed as a film, the IR measurements were carried out with the conventional NaCl disk method. A THF solution containing the desired components was cast onto an NaCl disk and dried under conditions

similar to those used in the bulk preparation. The film used in this study was sufficiently thin to obey the Beer–Lambert law. For a sample analyzed in solution, a permanently sealed cell with an NaCl window with a 0.05-mm path length (Wilmad) was used to study the equilibrium constant of the intermolecular interactions ($Ka$).

2D correlation analysis was conducted with Vector 3D software from Bruker Instrument Co. All spectra detected by 2D correlation analyses were normalized and classified into two sets, A and B. The spectra in set A are for pure POSS, 5/95 POSS/phenolic, 10/90 POSS/phenolic, 20/80 POSS/phenolic, and 30/70 POSS/phenolic. The spectra in set B are for 40/60 POSS/phenolic, 60/40 POSS/phenolic, and pure phenolic resin.

Shaded regions designate the negative intensity of the autopeaks or cross peaks in the 2D correlation spectrum. The unshaded regions designate positive intensities in the spectrum. The synchronous 2D spectrum was obtained to study the specific interactions between phenolic and POSS in the hybrid, whereas the asynchronous 2D IR spectrum was obtained to separate the bands of pure POSS from those of the phenolic/POSS hybrid.

### *WAXD*

X-ray diffraction spectra were collected on an X-ray diffraction instrument (M18XHF-SRA, MacScience Co., Japan) with Co K$\alpha$ radiation. Bragg's law ($\lambda = 2d \sin \theta$) was used to compute the spacing

### *Polarized Optical Microscopy*

The morphology of the hybrid material was monitored with an Olympus BH-651P polarized optical microscope. The sample was dissolved in THF and adsorbed on a glass plate by means of spin coating. The hybrid thin film was dried *in vacuo* at 40 °C for 24 h. The sample was melted by heating at 100 °C for 3 min and then cooled down slowly to room temperature over 20 min.

### *AFM Images*

A sample for AFM analysis was prepared by the spin-coating method by the casting of a sample with 20 wt % POSS content onto a glass plate. The hybrid thin film was dried *in vacuo* at 40 °C for 24 h. The surface morphology was recorded with the easyscan contact mode of an AFM system (Nanosurf AG). The spring constant of the cantilever was 5 N/m, and the feedback loop bandwidth was 12 kHz. All images were recorded under an air atmosphere at room temperature.

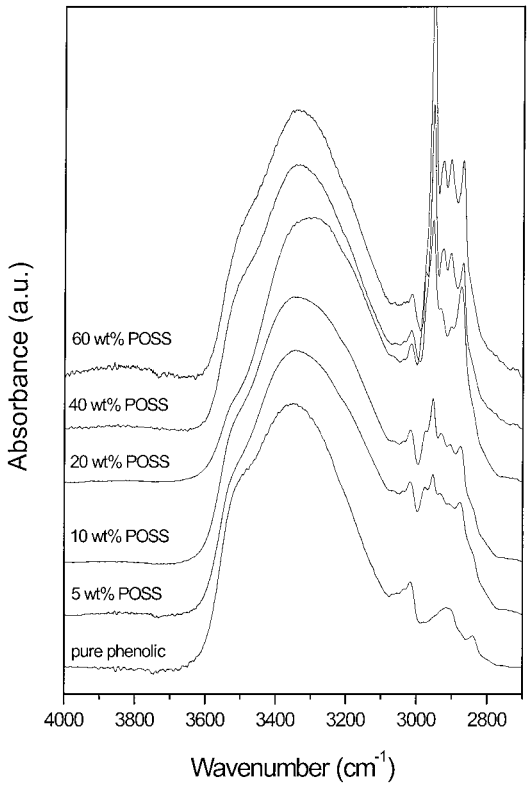


**Figure 1.** FTIR spectra recorded at room temperature from 2700 to 4000 $cm^{-1}$ for phenolic/POSS hybrids with various POSS contents.

## RESULTS AND DISCUSSION

### Analysis of One-Dimensional IR Spectra

Figure 1 displays the IR spectra measured at room temperature over the range of 2700–4000 $cm^{-1}$ of pure phenolic and various phenolic/POSS hybrids. The spectrum of the pure phenolic resin displays two hydroxyl components: a very broad band centered at 3350 $cm^{-1}$ that we attributed to a wide distribution of hydrogen-bonded hydroxyl groups and a relatively smaller shoulder band at 3525 $cm^{-1}$ that corresponds to free hydroxyl groups. The broad hydrogen-bonded hydroxyl band shifts to lower wave numbers with increasing POSS content and approaches a maximum shift to 3280 $cm^{-1}$ for the hybrid containing 20 wt % POSS [Fig. 1(d)]. In addition, the intensity of the signal of the free hydroxyl group is also

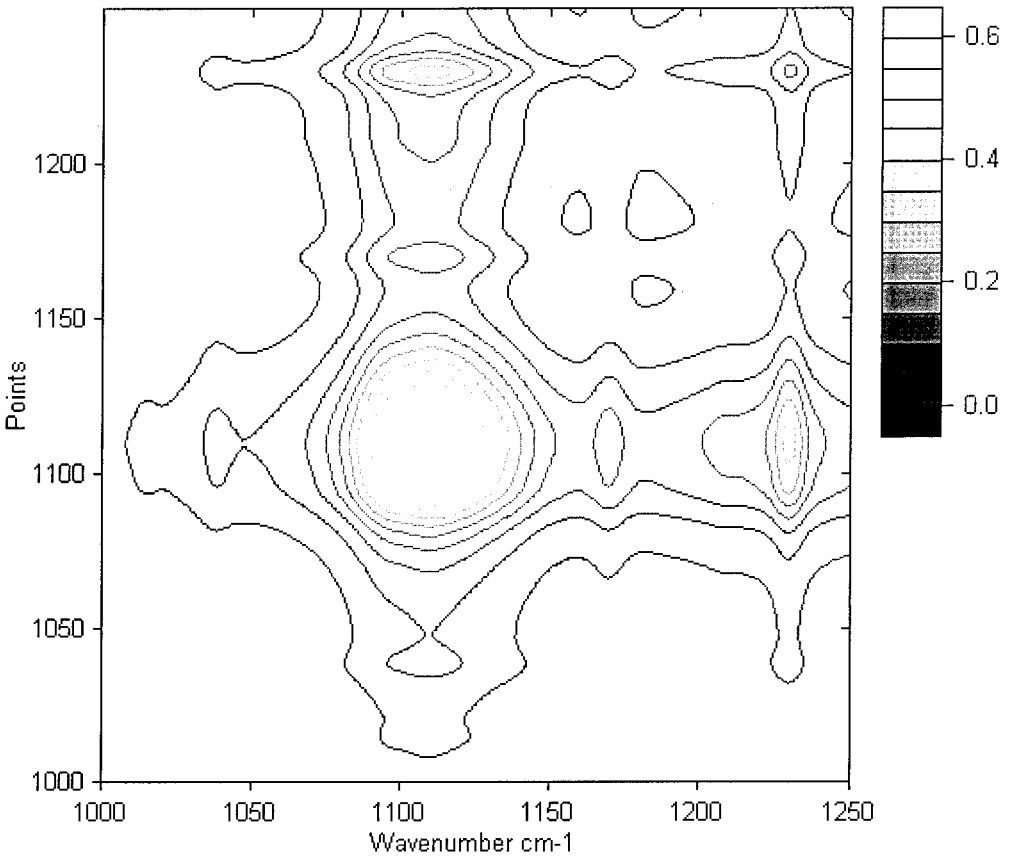


**Figure 2.** Synchronous 2D correlation map of set A in the region from 1000 to 1250 $cm^{-1}$.

minimized at a POSS content of 20 wt %. This change arises from a switch from intramolecular hydroxyl–hydroxyl bonding to intermolecular hydroxyl–siloxane hydrogen bonding, which indicates that hydrogen-bonding interactions exist between the phenolic hydroxyl group and the POSS siloxane group. When the POSS content is greater than 20%, however, the broad band for the hydrogen-bonded hydroxyl groups shifts back to a higher wave number and approaches a maximum wave number of 3350 $cm^{-1}$ for the hybrid containing 60 wt % POSS. Meanwhile, the intensity of the signal of the free hydroxyl group increases gradually with increasing POSS content but remains lower than that of pure phenolic. These observations suggest that the strength of intermolecular hydrogen bonding between POSS and phenolic tends to decrease at higher POSS contents (>20%) as the result of the aggregation of POSS, and so the blends tend to become less miscible; this results in macrophase separation of the POSS component in the phenolic matrix. Therefore, the behavior of the hydroxyl-stretching band of phenolic in the hybrid matrix tends to become akin to that of pure phenolic at a higher POSS content as a result of the macrophase separation occurring in this hybrid material. On the basis of IR spectroscopy, the strength of intermolecular hydrogen bonding within all these phenolic/POSS hybrids is greatest at a POSS content of 20 wt %.

### Analysis of 2D IR Spectra

Next, we turned our attention to the siloxane-stretching region of the phenolic/POSS hybrid. The Si—O—Si (siloxane) group absorption band of POSS, which appears at 1100 $cm^{-1}$, overlaps with the phenyl–OH stretching band of pure phenolic. The spectra are too complicated to allow us to assign the site of hydrogen bonding between POSS and phenolic. Therefore, we chose to use generalized 2D IR correlation spectroscopy to explore the hydrogen-bonding sites in phenolic/POSS hybrids. Figure 2 displays the synchronous 2D correlation map of set A in the range of 1250–

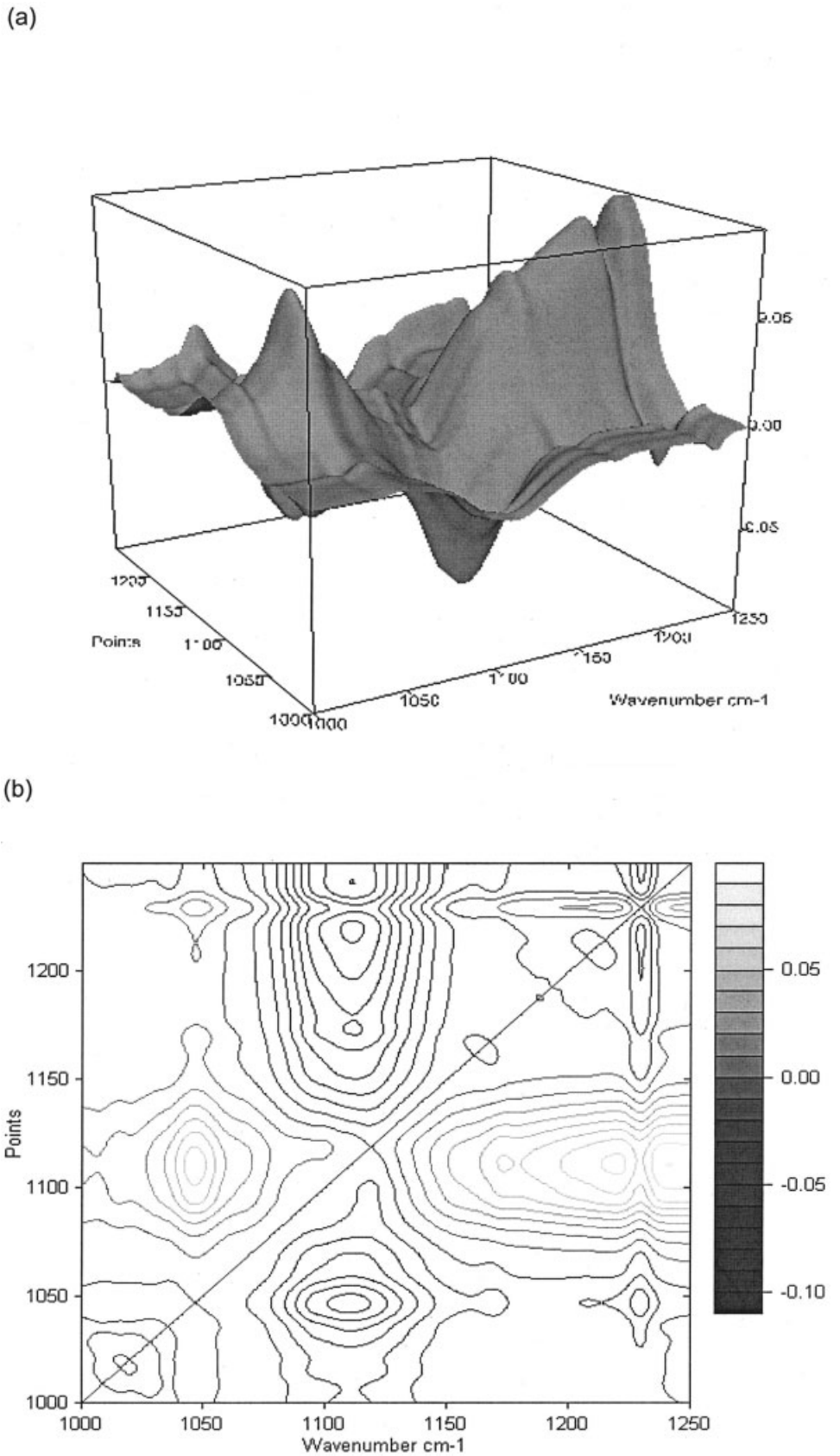


**Figure 3.** Asynchronous 2D correlation map of set A in the region from 1000 to 1250 $cm^{-1}$

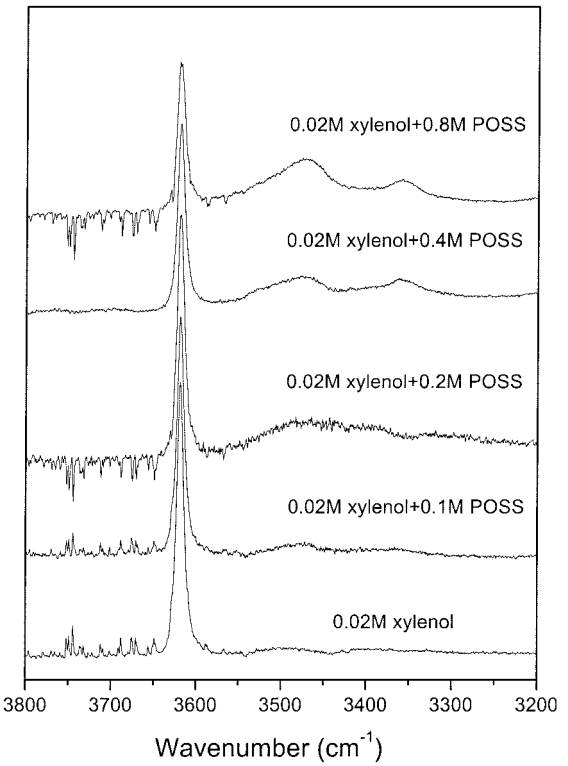


**Figure 4.** FTIR spectra displaying the band for the hydroxyl group stretching of 2,4-dimethylphenol in the presence of various concentrations of POSS.

1000 $cm^{-1}$. The characteristic absorption bands of POSS appear at 1100 and 1230 $cm^{-1}$, which correspond to the siloxane (Si—O—Si) and (Si—C) stretching vibrations, respectively. The characteristic absorption of phenolic is at 1223 $cm^{-1}$, which is the phenyl–OH stretching vibration. There are two positive cross peaks in Figure 2, which indicate that the hydrogen-bonding interaction occurs between the siloxane group of POSS (1100 $cm^{-1}$) and the phenyl–OH group (1223 $cm^{-1}$) of phenolic.

Figure 3(a,b) displays the asynchronous 2D correlation maps of the spectra of set A in the range of 1250–1000 $cm^{-1}$. The autopeak at 1100 $cm^{-1}$ splits into two separate POSS bands located at 1105 and 1160 $cm^{-1}$, which probably are due to two different siloxane (Si—O—Si) sites in the POSS cage. The one at a higher wave number is involved in hydrogen-bonding interactions with the hydroxyl group of phenolic, and the other, at a lower wave number, is the free siloxane. This result is similar to that observed in the case of water absorbed in a cured epoxy resin.[19]

Another autopeak at 1230 $cm^{-1}$ in Figure 3(a) also splits into two separate bands with opposite intensities, located at 1230 and 1220 $cm^{-1}$; this indicates that different polymer chains contribute to these two bands. The peak at 1230 $cm^{-1}$ arises from the Si—C stretching of POSS, and the peak at 1220 $cm^{-1}$ arises from the phenyl–OH stretching vibration of the phenolic resin. The positive cross peaks of the signals at 1220 and 1105 $cm^{-1}$ indicate that hydrogen-bonding interactions occur between the siloxane (Si—O—Si) group of POSS and the phenyl–OH group of the phenolic resin. When we consider the nature of ionic bonding in POSS, the isobutyl group can play a role either as an electron donor or, by donating to the unoccupied *d*-orbital of Si atoms, as an electron acceptor. The hydroxyl group of phenolic also acts as an electron donor through hydrogen bonding.

## Interassociation Equilibrium Constant Based on an Analysis with PCAM

According to PCAM, the interassociation equilibrium constant between a non-carbonyl group component and a hydrogen-bond-donating component can be calculated by the classical Coggesthall and Saier method.[20] Figure 4 displays the absorption hydroxyl group of 2,4-dimethylphenol (a model compound for phenolic) in cyclohexane containing different concentrations of POSS; the intensity of the absorption of the free hydroxyl group at 3620 $cm^{-1}$ decreases as the POSS concentration increases. The absolute intensity of the free hydroxyl group at 3620 $cm^{-1}$ can be considered a measurement of the number of free hydroxyl groups in the mixture. Figure 4 shows that the frequency of the band for the associated hydroxyl groups shifts from the free hydroxyl group at 3620 to 3490 $cm^{-1}$ as the concentration of POSS varies, as the result of hydrogen bonding between 2,4-dimethylphenol and POSS. The Coggesthall and Saier method can be expressed as follows:

**Table 1.** Values of $f_m^{OH}$ and *Ka* for Solutions of 2,4-Dimethylphenol in Cyclohexane with Various Concentractions of POSS

| Concentration of POSS (mol/L) | Intensity of IR Absorption | $f_m^{OH}$ | $Ka^{model}$ |
|---|---|---|---|
| 0 | 0.013 | 1 | — |
| 0.1 | 0.010 | 0.782 | 2.90 |
| 0.2 | 0.090 | 0.700 | 2.19 |
| 0.4 | 0.073 | 0.568 | 1.93 |
| 0.8 | 0.059 | 0.459 | 1.49 |

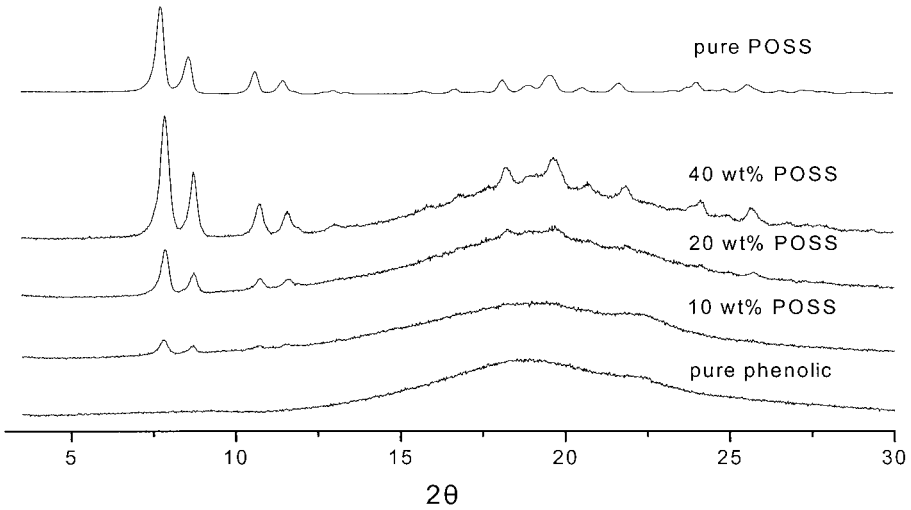


**Figure 5.** WAXD patterns in the range of $2\theta = 5$–$30°$ at various POSS concentrations.

$$Ka = \frac{1 - f_m^{OH}}{f_m^{OH}(C_A - (1 - f_m^{OH})C_B)} \quad (1)$$

where $C_A$ and $C_B$ denote the concentrations (mol $L^{-1}$) of POSS and 2,4-dimethylphenol, respectively, and $f_m^{OH}$ represents the fraction of free hydroxyl groups of 2,4-dimethylphenol. Table 1 lists the values of $f_m^{OH}$ for 2,4-dimethylphenol in the presence of various concentrations of POSS and the resulting values of $Ka$. The intrinsic value of $Ka$ of 3.21 L $mol^{-1}$ was obtained by the extrapolation of the POSS concentration to zero. The value of $Ka$ can be converted into $K_A$ by the division of the molar volume of the phenolic repeating unit (0.083 L $mol^{-1}$ at 25 °C).[13] In this manner, $K_A$ was calculated to be 38.67. From a previous study, we measured the self-association equilibrium constant of phenolic to be 52.3.[13] Clearly, the interassociation equilibrium constant of the phenolic/POSS blend is smaller than that of the self-association equilibrium constant of pure phenolic, and this indicates that the phenolic/POSS hybrid should be either partially miscible or immiscible because of the relatively poorer intermolecular association in comparison with that of the poly(vinyl phenol)/poly(acetoxystyrene)(PAS) blend system.

### Microstructure Analysis and the Self-Assembly Behavior of POSS

The morphologies of the phenolic/POSS hybrid materials were studied by WAXD to determine the microstructures of these hybrids as a function of the POSS content. The WAXD patterns of various phenolic/POSS blends are displayed in Figure 5. The pattern obtained with pure phenolic displaces a lack of crystallinity, with an amorphous halo appearing at $2\theta = 18.2$. The WAXD pattern of the pure POSS macromonomer with isobutyl hydrocarbon groups linked with silicon displays various strong peaks that indicate a crystalline structure. The intensity of the peaks of the crystalline structure increases with increasing POSS content in phenolic, and the positions of these peaks remain unchanged. The microstructures suggested by the WAXD patterns are consistent with the values of the interassociation and self-association equilibrium constants calculated from the IR spectra. The interassociation equilibrium constant between phenolic and POSS is lower than the strong self-association equilibrium constant of pure phenolic. These values imply that POSS is only partially miscible in phenolic and that it will aggregate at higher contents, as confirmed by the WAXD profiles.

The crystalline morphology and size were also investigated with polarized optical microscopy and atomic forced microscopy (AFM). Figure 6 displays the morphology obtained by polarized optical microscopy of the various phenolic/POSS hybrids. The crystalline phenolic/POSS hybrid material with a 20% POSS content has a narrow particle size distribution (1.5–2.0 $\mu$m), with the POSS particles arranged evenly in the phenolic matrix. At a higher POSS content (60 wt %), the crystalline POSS particles aggregate, and this leads to macrophase separation [Fig. 6(c)]. Furthermore, the crystal size of pure POSS in the absence of the phenolic resin is

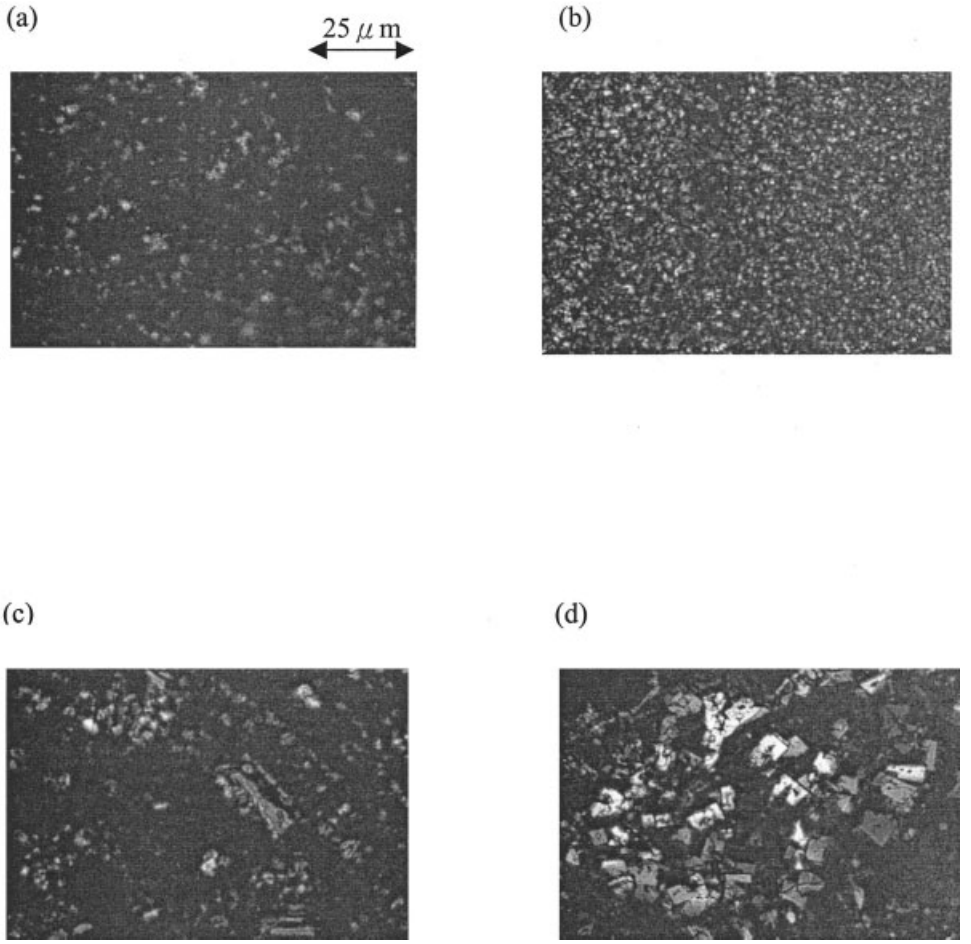


**Figure 6.** Polarized optical microscopy images of phenolic/POSS hybrids with various POSS contents: (a) 10 wt % POSS, (b) 20 wt % POSS, (c) 60 wt % POSS, and (d) pure POSS.

quite large [>20 $\mu$m; Fig. 6(d)]. These results suggest that crystalline POSS will tack on the surface of phenolic and that phenolic resin limits the growth of POSS crystals.

AFM was also used to investigate the surface morphologies of phenolic/POSS hybrids. The sample was prepared at a thickness of 2–4 $\mu$m via spin coating on a clear glass plate. Figure 7 displays the AFM images of the surfaces of pure phenolic and the 80/20 phenolic/POSS hybrid. Clearly, the surface image of the pure phenolic resin is homogeneous over an area of 7 $\mu$m $\times$ 7 $\mu$m. In contrast, the phenolic/POSS hybrid containing a POSS content of 20 wt % displays a nodal surface. The domain sizes of the POSS crystals are in the range of 1.5–2.0 $\mu$m, and the roughness of the surface is about 1 $\mu$m. The POSS crystals grow to a limited range of sizes in the phenolic matrix with a POSS content of 20 wt % as the result of the hydrogen-bonding interactions between POSS and phenolic phases. This AFM image confirms the self-assembly behavior of POSS.

## CONCLUSIONS

The miscibility, specific interaction, and self-assembly behaviors of phenolic/POSS hybrids were investigated by one-dimensional and 2D FTIR spectroscopy, WAXD, optical microscopy, and AFM. Hydrogen-bonding interactions were found in this phenolic/POSS hybrid system by an analysis of one-dimensional and 2D FTIR spectra. Furthermore, we calculated, using PCAM, the first interassociation equilibrium constant for this phenolic/POSS (organic–inorganic) hybrid system. The interassociation equilibrium constant in this phenolic/POSS hybrid is lower than the self-association equilibrium constant of pure phenolic. Macrophase separation occurs at a higher POSS content as a result of POSS aggregation. The phenolic/POSS hybrid material with a POSS content of 20 wt % possesses a structure in which crystalline POSS is arranged evenly in the phenolic matrix; the hydrogen bonding that exists

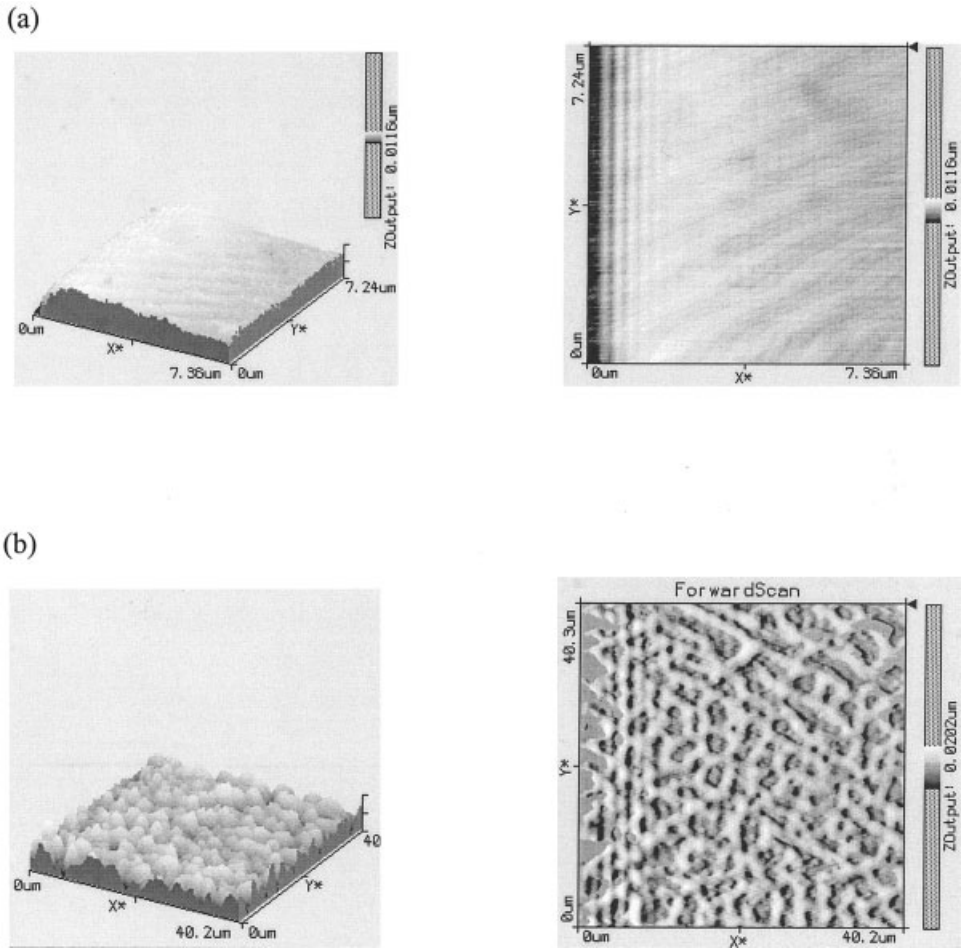


**Figure 7.** AFM images of the surface analysis of (a) pure phenolic and (b) a phenolic/POSS hybrid material with a POSS content of 20 wt %.

at the phenolic/POSS interface limits any further aggregation of POSS. The self-assembly behavior of the crystallization of POSS in this phenolic/POSS hybrid system was confirmed by WAXD, optical microscopy, and AFM analyses.

This research was supported financially by the National Science Council (Taiwan, Republic of China) under contract number NSC-91-2216-E-009-017.

## REFERENCES AND NOTES

1. Mather, P. T.; Jeon, H. G.; Romo-Uribe, A.; Haddad, T. S.; Lichtenhan, J. D. Macromolecules 1999, 32, 1194.
2. Choi, J.; Harcup, J.; Yee, A. F.; Zhu, Q.; Laine, R. M. J Am Chem Soc 2001, 123, 11420.
3. Haddad, S. T.; Lichtenhan, J. D. Macromolecules 1996, 29, 7302.
4. Zheng, L.; Farris, R. J.; Coughlin, E. B. Macromolecules 2001, 34, 8034.
5. Zheng, L.; Kasi, R. M.; Farris, R. J.; Coughlin, E. B. J Polym Sci Part A: Polym Chem 2002, 40, 885.
6. Zhang, C.; Laine, R. M. J Am Chem Soc 2000, 122, 6979.
7. Kim, K. M.; Chujo, Y. J Polym Sci Part A: Polym Chem 2001, 39, 4035.
8. Li, G. Z.; Wang, L.; Toghiani, H.; Daulton, T. L.; Koyama, K.; Pittman, U. Macromolecules 2001, 34, 8686.
9. Lichtenhan, J. D.; Otonari, Y. A.; Carr, M. J. Macromolecules 1995, 28, 8435.
10. Kim, K. M.; Keum, D. K.; Chujo, Y. Macromolecules 2003, 36, 867.
11. Sellinger, A.; Laine, R. M. Macromolecules 1996, 29, 2327.

12. Xu, H.; Kuo, S. W.; Lee, J. S.; Chang, F. C. Polymer 2002, 43, 5117.
13. Wu, H. D.; Chu, P. P.; Ma, C. C. M.; Chang, F. C. Macromolecules 1999, 32, 3097.
14. Kuo, S. W.; Lin, C. L.; Chang, F. C. Macromolecules 2002, 35, 278.
15. Noda, I. J Am Chem Soc 1989, 111, 8116.
16. Ren, Y.; Murakami, T.; Nishioka, T.; Nakashima, K.; Noda, I.; Ozaki, Y. Macromolecules 1999, 32, 6307.
17. Makashima, K.; Ren, Y.; Nishioka, T.; Tsubahara, N.; Noda, I.; Ozaki, Y. J Phys Chem B 1999, 103, 6704.
18. Coleman, M. M.; Graf, J. F.; Painter, P. C. Specific Interactions and the Miscibility of Polymer Blends; Technomic: Lancaster, PA, 1991.
19. Liu, M.; Wu, P.; Dinf, Y.; Chen, G.; Li, S. Macromolecules 2002, 35, 5500.
20. Coggesthall, N. D.; Saier, E. L. J Am Chem Soc 1951, 71, 5414.
21. Seifert, R.; Rytz, R.; Calzaferri, G. J Phys Chem A 2000, 104, 7473.
22. Bruhwiler, D.; Gfeller, N.; Calzaferri, G. J Phys Chem B 1998, 102, 2923.